Proceedings of IDETC/CIE 2013
ASME 2013 International Design Engineering Technical Conferences & Computers and Information in Engineering Conference
August 4 - 7, 2013, Portland, Oregon, USA

DRAFT DETC2013-13244

USING THE SINGULARITY TRACE TO UNDERSTAND LINKAGE MOTION CHARACTERISTICS

Lin Li
University of Dayton
Dayton, Ohio 45469
Email: lil4@udayton.edu

David H. Myszka*
University of Dayton
Dayton, Ohio 45469
Email: dmyszka1@udayton.edu

Andrew P. Murray
University of Dayton
Dayton, Ohio 45469
Email: amurray1@udayton.edu

Charles W. Wampler
General Motors R&D Center
Warren, Michigan 48090
Email: charles.w.wampler@gm.com

ABSTRACT

This paper provides examples of a new method used to analyze the motion characteristics of single-degree-of-freedom, closed-loop linkages with a designated input angle and one or two design parameters. The method involves the construction of a singularity trace, which is a plot that reveals changes in the number of geometric inversions, singularities, and changes in the number of branches as a design parameter is varied. This paper applies the method to Watt II, Stephenson III and double butterfly linkages. For the latter two linkages, instances where the input angle is able to rotate more than one revolution between singularities have been identified. This characteristic demonstrates a net-zero, singularity free, activation sequence that places the mechanism into a different geometric inversion. Additional observations from the examples are given. Instances where the singularity trace for Watt II linkages includes multiple coincident projections of the singularity curve. Cases are shown where subtle changes to two design parameters of a Stephenson III linkage drastically alters the motion. Additionally, isolated critical points are found to exist for the double butterfly, where the linkage becomes a structure and looses the freedom to move.

*Address all correspondence to this author.

1 Introduction

Myszka et al. [1] developed a general method to produce a *singularity trace* for a planar, single degree-of-freedom (DOF), closed-loop linkage with a designated input angle and a design parameter. The singularity trace can be a convenient tool to classify the general motion characteristics of a linkage with respect to changes in the design parameter. The motion characteristics include the number of geometric inversions, singularities, circuits and critical points, and are described as follows.

When the design parameter is considered fixed, forward kinematic position analysis determines values of the linkage joint parameters for a given position of the input link [2]. Since the governing kinematic constraint equations of a closed-loop linkage are non-linear, multiple solutions are obtained for a single position of the input link. Erdman et al., [3] refer to each solution as a *geometric inversion* (GI) and is associated with an alternate configuration of the linkage at the specific input. The set of position equations is represented by a motion curve which exhibits the relationship between the joint variables.

Chase and Mirth [4] define a *circuit* of a mechanism as the set of all possible orientations without disconnecting any of the joints. Each distinct segment on the trace of the motion curve represents a different circuit. When a GI is found to lie on a

segment of the motion curve at a specific input link position, any movement of the input link move the GI along that motion curve segment.

For a single-DOF linkage with a fixed design parameter, *singularity points* exist when the driving link is no longer able to move the mechanism. At the singularity points, also called dead points, the mechanism becomes locked and the mechanical advantage reduces to zero [5,6]. Singularities appear on the motion curve as turning points with respect to the input parameter. As the design parameter changes, these singularity points sweep out a curve called the singularity trace.

Regions on a circuit between singularity points are defined as *branches* [4]. For single-DOF linkages, singularity points are the input limits for that branch. If a GI resides on a motion curve segment (i.e., circuit) that has no singularities, it can be driven with a fully rotatable crank. As the design parameter changes, the number of branches and their connections, in short the topology of the motion curve, may change at certain critical points. *Critical points* are identified on the singularity trace as turning points with respect to the design parameter. Murray et al. [7] identified relationships of link lengths that defines a transition linkage as the border between topology. Myszka et al. [8] observed that critical points appearing as smooth extrema on the singularity trace are transition linkages. It was also observed that the Stephenson III linkage has the property that the input angle is able to rotate more than one revolution between singularities and this property is associated with critical points that appear as cusps on the singularity trace.

This paper illustrates the general analysis methodology for Watt II, Stephenson III and double butterfly linkages. The remainder of the paper is organized as follows. Section 2 applies the general method and develops governing equations for the Watt II linkage are developed. A singularity trace and associated observations for the Stephenson III is presented in Section 3. Section 4 develops the governing equations for the double butterfly linkage and provides observations from the resulting singularity trace.

2 Watt II Linkage

The Watt II linkage shown in Fig. 1 provides the first example. In the general analysis methodolgy, the linkage input variable is designated as $x \in \mathbb{C}$ and the design variable is $p \in \mathbb{C}$. All the remaining passive joint variables are $y \in \mathbb{C}^N$. For the Watt II linkage, the input angle is $x = \theta_1$ and the design parameter is $p = a_1$. The remaining passive joint variables are $y = \{\theta_2, \theta_3, \theta_6, \theta_7\}$. The physical parameters are θ_1, θ_4, α_{35}, and $a_2, \ldots, a_8$.

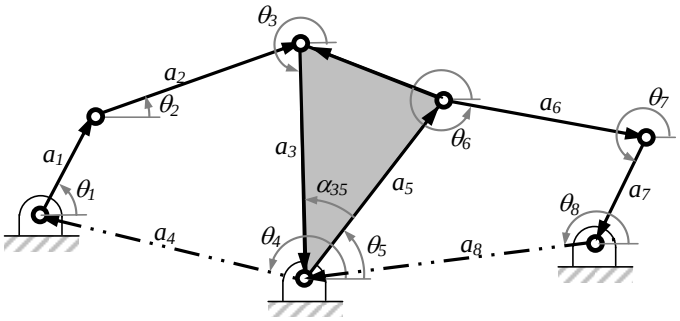

Figure 1: Watt II linkage position vector loop.

2.1 Loop Closure

The loop closure equations are specified as

$$f(p,x,y) = 0, \qquad f : \mathbb{C} \times \mathbb{C} \times \mathbb{C}^N \to \mathbb{C}^N. \tag{1}$$

For a fixed value of p, the mechanism has a single DOF motion represented by a motion curve $\mathcal{C}_p \subset \mathbb{C}^{N+1}$, $\dim(\mathcal{C}_p) = 1$.

To facilitate solution of loop closure equations, as presented in Wampler [9, 10], an isotropic form of loop closure equations are used. In isotropic form, each joint angle is represented by $\mathbf{T}_j = e^{i\theta_j} = \cos\theta_j + i\sin\theta_j$. The complex conjugate is $\overline{\mathbf{T}}_j = e^{-i\theta_j} = \cos\theta_j - i\sin\theta_j$, and the identity is $\mathbf{T}_j\overline{\mathbf{T}}_j = \left(e^{i\theta_j}\right)\left(e^{-i\theta_j}\right) = 1$. For the two loops in the Watt II linkage, the isotropic form of the closure condition along with the conjugate identities are

$$\begin{aligned}
g_1 &:= a_1\mathbf{T}_1 + a_2\mathbf{T}_2 + a_3\mathbf{T}_3 + a_4\mathbf{T}_4 = 0 \\
\bar{g}_1 &:= a_1\overline{\mathbf{T}}_1 + a_2\overline{\mathbf{T}}_2 + a_3\overline{\mathbf{T}}_3 + a_4\overline{\mathbf{T}}_4 = 0 \\
g_2 &:= b_5\mathbf{T}_3 + a_6\mathbf{T}_6 + a_7\mathbf{T}_7 + a_8\mathbf{T}_8 = 0 \\
\bar{g}_2 &:= b_5'\overline{\mathbf{T}}_3 + a_6\overline{\mathbf{T}}_6 + a_7\overline{\mathbf{T}}_7 + a_8\overline{\mathbf{T}}_8 = 0 \\
h_j &:= \mathbf{T}_j\overline{\mathbf{T}}_j - 1 = 0, \qquad j = 2,3,6,7
\end{aligned} \tag{2}$$

All of the a_j are real link lengths, but b_5 is a complex stretch rotation to properly model the ternary link. That is, $b_5 = a_5(\cos\alpha_{35} + i\sin\alpha_{35})$, and b_5' is the complex conjugate of b_5. Note that $\mathbf{T}_4, \overline{\mathbf{T}}_4$ and $\mathbf{T}_8, \overline{\mathbf{T}}_8$ model the ground link and are known. For a fixed design variable, the system of four equations describes a curve in the four dimensional space of $\{\mathbf{T}_2, \mathbf{T}_6, \overline{\mathbf{T}}_2, \overline{\mathbf{T}}_6\}$. In the numerical examples that follow, the values used for the physical parameters are: $a_2 = 4.5$, $a_3 = 5.0$, $a_4 = 6.0$, $a_5 = 4.5$, $a_6 = 2.5$, $a_7 = 2.0$, $a_8 = 5.5$, $\theta_4 = 3.1416$, $\theta_8 = 3.9270$, $\alpha_{35} = 0.5236$.

2.2 Forward Kinematics

Since the loop equations, g_1, g_2, and the conjugate loop equations, $\bar{g}_1, \bar{g}_1$ are all linear, Eq. 2 can be rewritten to eliminate variables. To this end, two variables per loop are eliminated by defining,

$$\begin{aligned}
\mathbf{R}_2 &:= -a_2\mathbf{T}_2 = a_1\mathbf{T}_1 + a_3\mathbf{T}_3 + a_4\mathbf{T}_4, \\
\overline{\mathbf{R}}_2 &:= -a_2\overline{\mathbf{T}}_2 = a_1\overline{\mathbf{T}}_1 + a_3\overline{\mathbf{T}}_3 + a_4\overline{\mathbf{T}}_4, \\
\mathbf{R}_7 &:= -a_7\mathbf{T}_7 = b_5\mathbf{T}_3 + a_6\mathbf{T}_6 + a_8\mathbf{T}_8, \\
\overline{\mathbf{R}}_7 &:= -a_7\overline{\mathbf{T}}_7 = b_5'\overline{\mathbf{T}}_3 + a_6\overline{\mathbf{T}}_6 + a_8\overline{\mathbf{T}}_8.
\end{aligned} \tag{3}$$

With $a_i \neq 0$, $i = 2, 7$, $a_i^2 h_i = 0$ is formed to achieve

$$H_2 = \mathbf{R}_2\overline{\mathbf{R}}_2 - a_2^2 = 0, \tag{4}$$
$$H_7 = \mathbf{R}_7\overline{\mathbf{R}}_7 - a_7^2 = 0. \tag{5}$$

The identities corresponding to the remaining joint variables are

$$h_1 = \mathbf{T}_1\overline{\mathbf{T}}_1 - 1 = 0, \tag{6}$$
$$h_3 = \mathbf{T}_3\overline{\mathbf{T}}_3 - 1 = 0, \tag{7}$$
$$h_6 = \mathbf{T}_6\overline{\mathbf{T}}_6 - 1 = 0, \tag{8}$$
$$\tag{9}$$

For forward kinematics, the input angle θ_1 is given, and therefore $\mathbf{T}_1$ and $\overline{\mathbf{T}}_1$ are known and Eq. 6 is not used. The forward kinematics solutions are the roots of Eqs. (4),(5),(7),(8), a system of four bilinear equations in the two-homogeneous variable groups $\{\mathbf{T}_3, \mathbf{T}_6\}$,$\{\overline{\mathbf{T}}_3, \overline{\mathbf{T}}_6\}$. Solution of the polynomial systems can be readily accomplished by numerical polynomial continuation [11] using the Bertini software package [12]. "Real" solutions are those for which $|\mathbf{T}_3| = |\mathbf{T}_6| = 1$. At any point on the curve, the remaining angles can be solved by using

$$\mathbf{T}_2 = -\mathbf{R}_2/a_2, \quad \mathbf{T}_7 = -\mathbf{R}_7/a_7. \tag{10}$$

2.3 Singularity Points

Given a linkage with a fixed design parameter, it is desirable to find all branches of the motion with respect to the designated input parameter. As described in [4], the branches meet at the singularity points of the curve, where the mechanism moves differentially without any motion at the input. The mechanism is locked at a singularity point, but can be driven smoothly from the input along each motion branch. The singularity points occur when $\Delta y \neq 0$ with $\Delta x = 0$, which implies that the Jacobian of the loop equations with respect to the passive joint variables loses rank

$$D(p,x,y) := \det \frac{\partial f}{\partial y} = 0. \tag{11}$$

Accordingly, the singularity points are given by a system of equations consisting of the five loop closure conditions Eqs. (6)–(8) along with one additional condition,

$$D := \det \begin{bmatrix} \frac{\partial H_2}{\partial \theta_3} & \frac{\partial H_2}{\partial \theta_6} \\ \frac{\partial H_7}{\partial \theta_3} & \frac{\partial H_7}{\partial \theta_6} \end{bmatrix}. \tag{12}$$

It is noted that $\frac{\partial H_2}{\partial \theta_6} = 0$ since $\mathbf{T}_6$ does not appear in $\mathbf{R}_2$. This system of six equations in the six unknowns, separated into two-homogeneous variable groups $\{\mathbf{T}_1, \mathbf{T}_2, \mathbf{T}_6\}, \{\overline{\mathbf{T}}_1, \overline{\mathbf{T}}_2, \overline{\mathbf{T}}_6\}$. Solving the system using Bertini [12], at most 8 turning points are found in a general example. When $a_1 = 2.0$, 2 of 16 singularity points are real. When $a_1 = 6.0$ and $a_1 = 12.0$, 4 of 16 singularity points are real. When $a_1 = 9.0$, 6 of 16 singularity points are real.

2.4 Motion Curve

A trace of a motion curve with $a_1 = 2.0$ is projected onto the θ_1 - θ_6 plane and shown in Fig. 2. Note that the linkage has one circuit and two singularity points at $\theta_1 = -0.2061, 2.0652$. Zero GIs exist for $\theta_1 < -0.2061$ and $\theta_1 > 2.0652$. Two GIs exist for $-0.2061 < \theta_1 < 2.0652$.

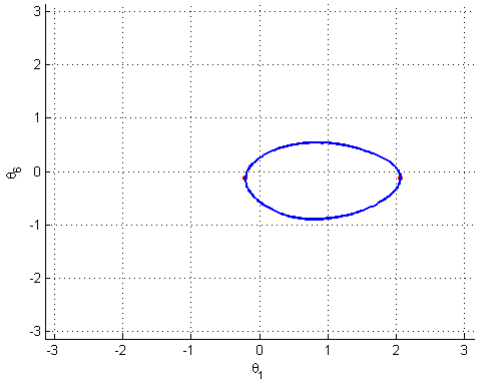

Figure 2: Trace of the motion curve for the Watt II linkage, with $a_1 = 2.0$, projected onto the $\theta_1 - \theta_6$ plane.

A second trace of a motion curve with $a_1 = 9.0$ is projected onto the θ_1 - θ_6 plane and shown in Fig. 3. Note the motion curve has two circuits and six of singularity points at $\theta_1 = -0.2427$, 0.6019, 0.6314, 1.2277, 1.3205, 1.3205. Notice that two singulatiries occur at the same value of θ_1. This is associated with singularity within the first four-bar loop, for which two inversions of the second four-bar loop exist. The linkage has zero GIs for $\theta_1 < -0.2427$, $0.6019 < \theta_1 < 0.6314$ and $\theta_1 > 1.3205$. Two

GIs exist for $-0.2427 < \theta_1 < 0.6019$ and $0.6314 < \theta_1 < 1.227$
Four GIs exist for all values of $1.2277 < \theta_1 < 1.3205$.

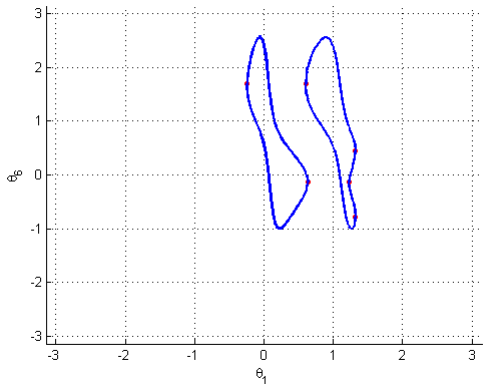

Figure 3: Trace of the motion curve for the Watt II linkage, with $a_1 = 9.0$, projected onto the $\theta_1 - \theta_6$ plane.

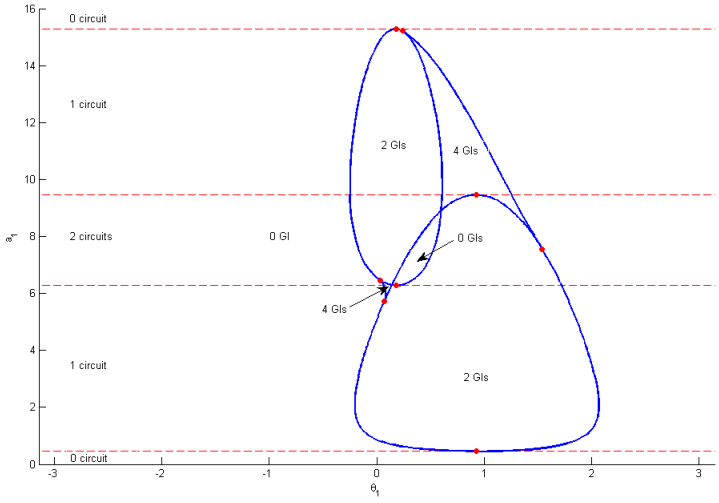

Figure 4: Projection of the Watt II singularity trace. Red circles mark the critical points. Regions of equal GIs and circuits are identified.

2.5 Critical Points

The process of determining the critical points proceeds analogously to finding singularity points, replacing x by p, y by (x,y), and f by (f,D). The critical points occur when $(\Delta x, \Delta y) \neq 0$ with $\Delta p = 0$, which implies,

$$E := \det \begin{bmatrix} \frac{\partial f}{\partial x} & \frac{\partial f}{\partial y} \\ \frac{\partial D}{\partial x} & \frac{\partial D}{\partial y} \end{bmatrix} = 0. \tag{13}$$

Considering a_1 as a variable, the critical points for the Watt II are determined by the solution of Eq. (6)–(5),(12) along with,

$$E := \det \begin{bmatrix} \frac{\partial H_2}{\partial \theta_1} & \frac{\partial H_2}{\partial \theta_3} & \frac{\partial H_2}{\partial \theta_6} \\ \frac{\partial H_7}{\partial \theta_1} & \frac{\partial H_7}{\partial \theta_3} & \frac{\partial H_7}{\partial \theta_6} \\ \frac{\partial D}{\partial \theta_1} & \frac{\partial D}{\partial \theta_3} & \frac{\partial D}{\partial \theta_6} \end{bmatrix} = 0. \tag{14}$$

It is noted that $\frac{\partial H_2}{\partial \theta_6} = 0$, since $\mathbf{T}_6$ does not appear in $\mathbf{R}_2$, and $\frac{\partial H_7}{\partial \theta_1} = 0$, since $\mathbf{T}_1$ does not appear in $\mathbf{R}_7$. This system of seven equations in the seven unknowns a_1,$\{\mathbf{T}_1, \mathbf{T}_2, \mathbf{T}_6\}$,$\{\overline{\mathbf{T}}_1, \overline{\mathbf{T}}_2, \overline{\mathbf{T}}_6\}$. Using Bertini to solve, critical points appear in pairs, existing at a_1 = 0.4614, 5.7107, 6.2872, 6.4642, 7.5578, 9.4614, 15.2132, 15.2872.

2.6 Singularity Trace

The singularity trace is shown in Fig. 4. The critical points signify local extrema of the singularity curve. Cricital points that appear on the singularity trace as smooth extrema represent transition linkages, where there is a change in the number of circuits.

Sampling the motion curve between critical points determines the number of circuits. As identified in [8], the singularity trace separates the plot into zones having the same number of GIs. Solving the forward kinematic problem for one sample point within each zone determines the number in GIs in the zone, as indicated in Fig. 4. It commonly occurs that the number of GIs in adjacent regions differ by two. With the symmetry in the Watt II motion curves, some of the arcs observed on the singularity trace are actually two coincident arcs. As mentioned, this is associated with a singularity within the first four-bar loop, for which two GIs of the second four-bar loop exist for the same input angle. In these cases, the number of GIs in adjacent regions differ by four, as is seen in the upper right portion of this singularity trace.

3 Stephenson III Linkage

For the Stephenson III shown in Fig. 5, $x = \theta_1$ is considered the input angle and the design parameter is designated as $p = a_1$. The remaining joint variables are $y = \{\theta_2, \theta_3, \theta_6, \theta_7\}$. The physical parameters are θ_1, θ_4, α_{35}, and $a_2, \ldots, a_8$. In the numerical examples that follow, the values used for the physical parameters are: $a_2 = 4.0$, $a_3 = 3.5$, $a_4 = 4.1$, $a_5 = 8.0$, $a_6 = 8.0$, $a_7 = 8.0$, $a_8 = 5.0$, $\theta_5 = 1.5708$, $\theta_6 = 5.8832$, and $\alpha_{38} = 0.7752$. The governing loop, singularity and critical point equations were developed in [1], so only the resulting equations are presented

here. The loop closure equations are

$$\begin{aligned}
\mathbf{R}_2 &:= a_2\mathbf{T}_2 = -(a_1\mathbf{T}_1 + a_3\mathbf{T}_3 + a_4\mathbf{T}_4 + a_5\mathbf{T}_5),\\
\overline{\mathbf{R}}_2 &:= a_2\overline{\mathbf{T}}_2 = -(a_1\overline{\mathbf{T}}_1 + a_3\overline{\mathbf{T}}_3 + a_4\overline{\mathbf{T}}_4 + a_5\overline{\mathbf{T}}_5),\\
\mathbf{R}_7 &:= a_7\overline{\mathbf{T}}_7 = -(b_3\mathbf{T}_3 + a_4\mathbf{T}_4 + a_6\mathbf{T}_6),\\
\overline{\mathbf{R}}_7 &:= a_7\overline{\mathbf{T}}_7 = -(b_3'\overline{\mathbf{T}}_3 + a_4\overline{\mathbf{T}}_4 + a_6\overline{\mathbf{T}}_6),
\end{aligned} \tag{15}$$

Using (15), the closure conditions become

$$h_1 = \mathbf{T}_1\overline{\mathbf{T}}_1 - 1 = 0, \tag{16}$$
$$H_2 = \mathbf{R}_2\overline{\mathbf{R}}_2 - a_2^2 = 0, \tag{17}$$
$$h_3 = \mathbf{T}_3\overline{\mathbf{T}}_3 - 1 = 0, \tag{18}$$
$$h_4 = \mathbf{T}_4\overline{\mathbf{T}}_4 - 1 = 0, \tag{19}$$
$$H_7 = \mathbf{R}_7\overline{\mathbf{R}}_7 - a_7^2 = 0. \tag{20}$$

The singularity condition is

$$D := \det\begin{bmatrix} \frac{\partial H_2}{\partial\theta_3} & \frac{\partial H_2}{\partial\theta_4} \\ \frac{\partial H_7}{\partial\theta_3} & \frac{\partial H_7}{\partial\theta_4} \end{bmatrix} = 0. \tag{21}$$

Lastly, the condition for critical points is

$$E := \det\begin{bmatrix} \frac{\partial H_2}{\partial\theta_1} & \frac{\partial H_2}{\partial\theta_3} & \frac{\partial H_2}{\partial\theta_4} \\ 0 & \frac{\partial H_7}{\partial\theta_3} & \frac{\partial H_7}{\partial\theta_4} \\ \frac{\partial D}{\partial\theta_1} & \frac{\partial D}{\partial\theta_3} & \frac{\partial D}{\partial\theta_4} \end{bmatrix} = 0. \tag{22}$$

3.1 Critical Points

The system of equations for determination of critical points consists of Eqs. (16)–(20),(21),(22). Considering a_1 as a variable design paramater, this system of seven equations in the seven unknowns grouped into the homogenous system a_1,$\{\mathbf{T}_1,\mathbf{T}_3,\mathbf{T}_4\}$,$\{\overline{\mathbf{T}}_1,\overline{\mathbf{T}}_3,\overline{\mathbf{T}}_4\}$. Using Bertini to solve, critical points exist at a_1 = 1.1114, 2.0471, 2.0551, 5.9129, 5.9529, 5.9728, 7.4384, 7.5190, 8.7611, 8.8284, 10.0551, 10.9436, 13.7642, 13.9129, 17.4641, 18.9436.

3.2 Singularity trace

The singularity trace with a_1 as a variable is shown in Fig. 6. Unlike the Watt II linkage, some critical points appear as cusps on the singularity trace. Solving the forward kinematic problem for one sample point within each region bounded by the singularity curve determines the number of GIs in that entire region. The number of GIs are noted in Fig. 6. Additionally, the number of circuits changes by one at each non-cusp, extrema and are also noted in Fig. 6.

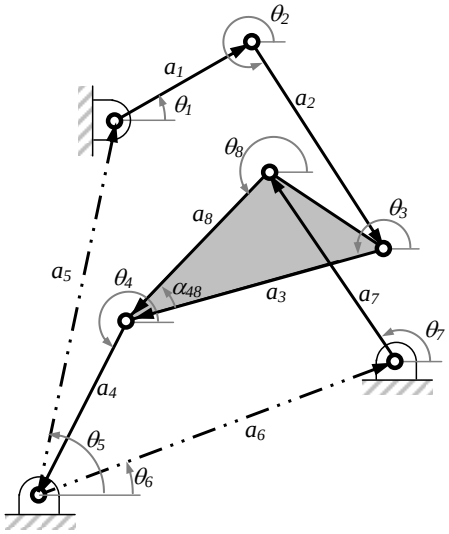

Figure 5: Stephenson III linkage position vector loop.

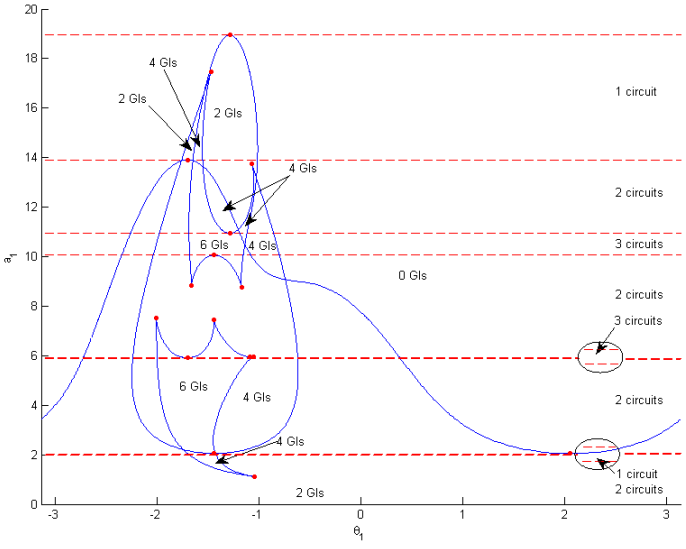

Figure 6: Projection of the Stephenson III singularity trace with respect to a_1. Red circles mark the critical points. Regions of equal GIs and circuits are identified.

3.3 Motion Curves

A trace of the motion curve with $a_1 = 1.1$ is projected onto the θ_1- θ_3 plane and shown in Fig. 7. This value of a_1 is slightly less than the smallest critial point value (1.1114). Note that this lowest cricital point appears as a cusp in Fig. 6. This linkage has two GIs for all values of θ_1, two separate circuits and no singularities. Thus, two linkage configurations have continuously rotating cranks with $a_1 < 1.1114$.

A second trace of the motion curve with $a_1 = 2.0$ is projected onto the θ_1- θ_3 plane and shown in Fig. 8. This value of a_1 is slightly greater than the smallest critial point value (1.1114). This linkage has two GIs for $\theta_1 < -1.6902$ and $\theta_1 > -1.4259$, four GIs for $-1.6902 < \theta_1 < -1.4259$, two separate circuits and two singularities. The change of a_1 from 1.1 to 2.0 passes over a cusp in Fig. 6 and two singularities are introduced without additional circuit. Thus, the motion curve bends over itself as seen in Fig. 8. This results in a linkage that is able to rotate greater than one full revolution between singularities. As observed in [1] and witnessed again here, this net-zero, singularity-free actuation that places the linkage into a different GI is associated with cusps on the singularity trace.

The following analysis considers changes in two design parameters. The motion curve shown in Fig. 8 was generated with $a_1 = 2.00$ and $a_4 = 4.10$ and exhibited two circuits, one having a fully rotating crank and the other containing a greater than 360° branch. Figure 9 shows a pair of singulatiry traces with a_4 considered variable. The solid trace is with $a_1 = 2.00$ and the dashed trace is with $a_1 = 2.09$. Adjusting a_1 from 2.00 to 2.09 crosses a critical point in Fig. 6. Additionally, adjusting a_4 from 4.10 to 4.15 crosses the critical point on both traces in Fig. 9. The motion curve shown in Fig. 10 was generated with $a_1 = 2.09$ and $a_4 = 4.15$. After making both subtle adjustments, the two circuits in Fig. 8 have been merged and no GI is fillu able to rotate. Moreover, an additional circuit with two branches has been formed. Thus, subtle adjustments to two link lengths, each crossing a corresponding critical point, results in drastically different motion characterisitcs.

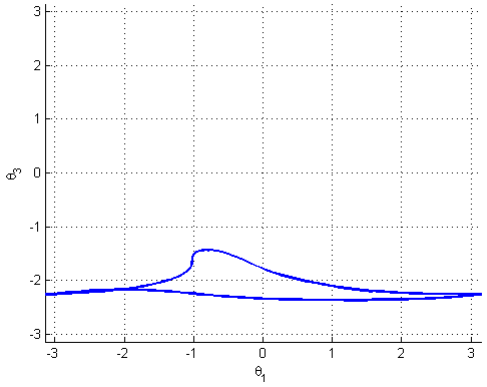

Figure 7: Stephenson III Linkage motion curve with respect to θ_1, θ_3 at $a_1 = 1.1$.

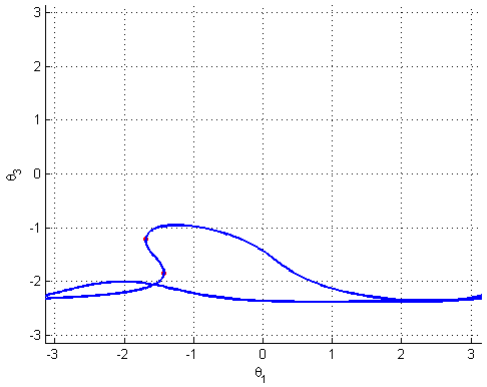

Figure 8: Stephenson III Linkage motion curve with respect to θ_1, θ_3 at $a_1 = 2.0$.

4 Double Butterfly Linkage

This section applies the general analysis methodology to the double butterfly linkage, as shown in Fig. 11. For this case, the input angle is $x = \theta_1$ and the design parameter is designated as $p = a_1$. The remaining joint variables are $y = \{\theta_2, \theta_3, \theta_4, \theta_7, \theta_8, \theta_{11}\}$. The physical parameters are θ_1, θ_5, θ_{12}, α_2, α_4, α_7, and $a_2, \ldots, a_{12}$.

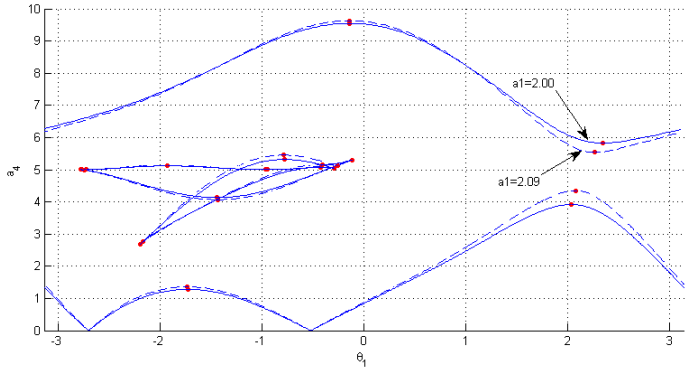

Figure 9: Stephenson III singularity trace with respect to a_4.

4.1 Loop Closure

The double butterfly linkage has three loops. The isotropic form of the loop closure conditions for the double butterfly link-

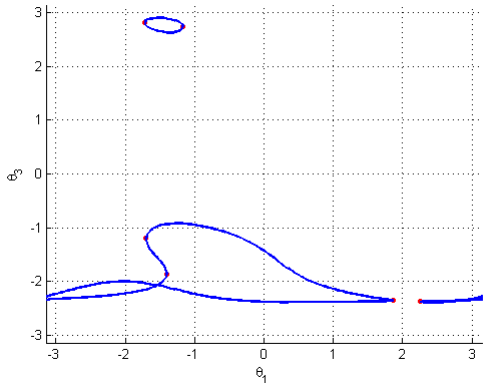

Figure 10: Stephenson III singularity trace with respect to $a_1 = 2.09, a_4 = 4.15$.

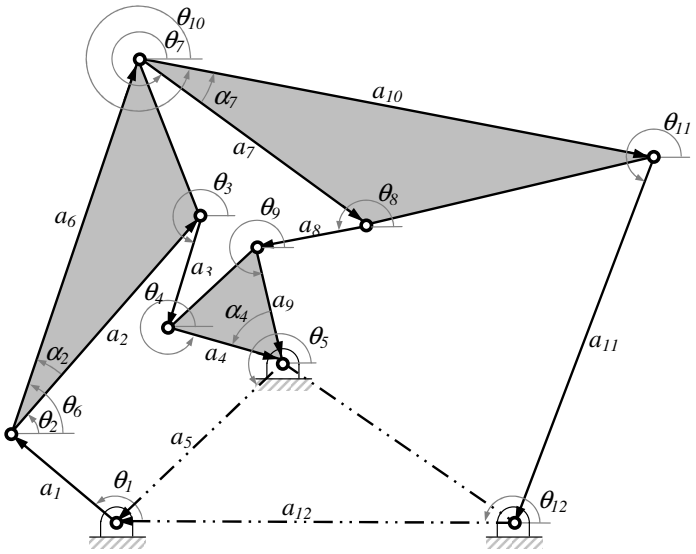

Figure 11: Double butterfly linkage position vector loop.

age can be written as

$$
\begin{aligned}
g_1 &:= a_1\mathbf{T}_1 + a_2\mathbf{T}_2 + a_3\mathbf{T}_3 + a_4\mathbf{T}_4 + a_5\mathbf{T}_5 = 0,\\
\bar{g}_1 &:= a_1\overline{\mathbf{T}}_1 + a_2\overline{\mathbf{T}}_2 + a_3\overline{\mathbf{T}}_3 + a_4\overline{\mathbf{T}}_4 + a_5\overline{\mathbf{T}}_5 = 0,\\
g_2 &:= a_1\mathbf{T}_1 + b_6\mathbf{T}_2 + a_7\mathbf{T}_7 + a_8\mathbf{T}_8 + b_9\mathbf{T}_4 + a_5\mathbf{T}_5 = 0,\\
\bar{g}_2 &:= a_1\overline{\mathbf{T}}_1 + b_6'\overline{\mathbf{T}}_2 + a_7\overline{\mathbf{T}}_7 + a_8\overline{\mathbf{T}}_8 + b_9'\overline{\mathbf{T}}_4 + a_5\overline{\mathbf{T}}_5 = 0,\\
g_3 &:= a_1\mathbf{T}_1 + b_6\mathbf{T}_2 + b_{10}\mathbf{T}_7 + a_{11}\mathbf{T}_{11} + a_{12}\mathbf{T}_{12} = 0,\\
\bar{g}_3 &:= a_1\overline{\mathbf{T}}_1 + b_6'\overline{\mathbf{T}}_2 + b_{10}'\overline{\mathbf{T}}_7 + a_{11}\overline{\mathbf{T}}_{11} + a_{12}\overline{\mathbf{T}}_{12} = 0,\\
h_j &:= \mathbf{T}_j\overline{\mathbf{T}}_j - 1 = 0, \qquad j = 2,3,4,7,8,11.
\end{aligned}
\tag{23}
$$

As before, all of the a_j are real link lengths, but b_6, b_9, b_{10} are the complex stretch rotations to properly model the ternary links. That is, $b_6 = a_6(\cos\alpha_2 + i\sin\alpha_2)$, $b_9 = a_9(\cos\alpha_4 + i\sin\alpha_4)$, $b_{10} = a_{10}(\cos\alpha_7 + i\sin\alpha_7)$, and b_6', b_9', b_{10}' are the complex conjugates of b_6, b_9, b_{10}. The system of twelve equations in Eqs. 23 describes a curve in the twelve-dimensional space of $\{\mathbf{T}_2, \mathbf{T}_3, \mathbf{T}_4, \mathbf{T}_7, \mathbf{T}_8, \mathbf{T}_{11}, \overline{\mathbf{T}}_2, \overline{\mathbf{T}}_3, \overline{\mathbf{T}}_4, \overline{\mathbf{T}}_7, \overline{\mathbf{T}}_8, \overline{\mathbf{T}}_{11}\}$. In the numerical examples that follow, the values used for the physical parameters are: $a_2 = 5.0$, $a_3 = 2.0$, $a_4 = 2.0$, $a_5 = 4.0$, $a_6 = 7.0$, $a_7 = 5.0$, $a_8 = 2.0$,$a_9 = 2.0$, $a_10 = 9.0$, $a_11 = 7.0$, $a_12 = 7.0$, $\theta_5 = 3.9168$, $\theta_{12} = 3.1416$, $\alpha_4 = 1.0472$, $\alpha_2 = 0.3803$ and $\alpha_7 = 0.4510$.

4.2 Forward Kinematics

The forward kinematic problem considers $p = a_1$ fixed, the passive joint variables are determined for a given input θ_1. Some variables can be eliminated from Eqs. (23) to facilitate solution,

$$
\begin{aligned}
\mathbf{R}_3 &:= -a_3\mathbf{T}_3 = a_1\mathbf{T}_1 + a_2\mathbf{T}_2 + a_4\mathbf{T}_4 + a_5\mathbf{T}_5,\\
\overline{\mathbf{R}}_3 &:= -a_3\overline{\mathbf{T}}_3 = a_1\overline{\mathbf{T}}_1 + a_2\overline{\mathbf{T}}_2 + a_4\overline{\mathbf{T}}_4 + a_5\overline{\mathbf{T}}_5,\\
\mathbf{R}_8 &:= -a_8\mathbf{T}_8 = a_1\mathbf{T}_1 + b_6\mathbf{T}_2 + a_7\mathbf{T}_7 + b_9\mathbf{T}_4 + a_5\mathbf{T}_5,\\
\overline{\mathbf{R}}_8 &:= -a_8\overline{\mathbf{T}}_8 = a_1\overline{\mathbf{T}}_1 + b_6'\overline{\mathbf{T}}_2 + a_7\overline{\mathbf{T}}_7 + b_9\overline{\mathbf{T}}_4 + a_5\overline{\mathbf{T}}_5,\\
\mathbf{R}_{11} &:= -a_{11}\mathbf{T}_{11} = a_1\mathbf{T}_1 + b_6\mathbf{T}_2 + b_{10}\mathbf{T}_7 + a_{12}\mathbf{T}_{12},\\
\overline{\mathbf{R}}_{11} &:= -a_{11}\mathbf{T}_{11} = a_1\overline{\mathbf{T}}_1 + b_6'\overline{\mathbf{T}}_2 + b_{10}'\overline{\mathbf{T}}_7 + a_{12}\overline{\mathbf{T}}_{12}.
\end{aligned}
\tag{24}
$$

Accordingly, for $a_i \neq 0$, $i = 3, 8, 11$, $a_i^2 h_i = 0$ is formed to achieve

$$H_3 := \mathbf{R}_3\overline{\mathbf{R}}_3 - a_3^2 = 0, \tag{25}$$
$$H_8 := \mathbf{R}_8\overline{\mathbf{R}}_8 - a_8^2 = 0, \tag{26}$$
$$H_{11} := \mathbf{R}_{11}\overline{\mathbf{R}}_{11} - a_{11}^2 = 0. \tag{27}$$

The identities corresponding to the remaining the joint valuables are

$$h_2 := \mathbf{T}_2\overline{\mathbf{T}}_2 - 1 = 0, \tag{28}$$
$$h_4 := \mathbf{T}_4\overline{\mathbf{T}}_4 - 1 = 0, \tag{29}$$
$$h_7 := \mathbf{T}_7\overline{\mathbf{T}}_7 - 1 = 0, \tag{30}$$

For a given design, the solution of this system of six Eqs. (25)-(30) in the six unknowns, separated into two-homogeneous variable groups $\{\mathbf{T}_2, \mathbf{T}_4, \mathbf{T}_7\}$,$\{\overline{\mathbf{T}}_2, \overline{\mathbf{T}}_4, \overline{\mathbf{T}}_7\}$ is the motion curve of the linkage. As before, "real" solutions are those for which $|\mathbf{T}_2| = |\mathbf{T}_4| = |\mathbf{T}_7| = 1$. At any point on the curve, the

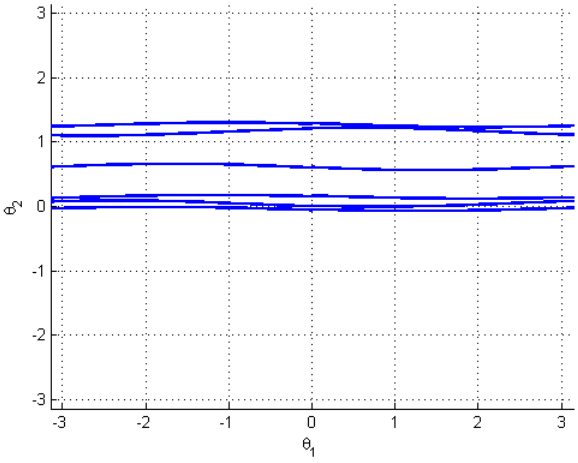

Figure 12: Trace of the motion curve for the double butterfly linkage, with $a_1 = 0.198$, projected onto the $\theta_1 - \theta_2$ plane.

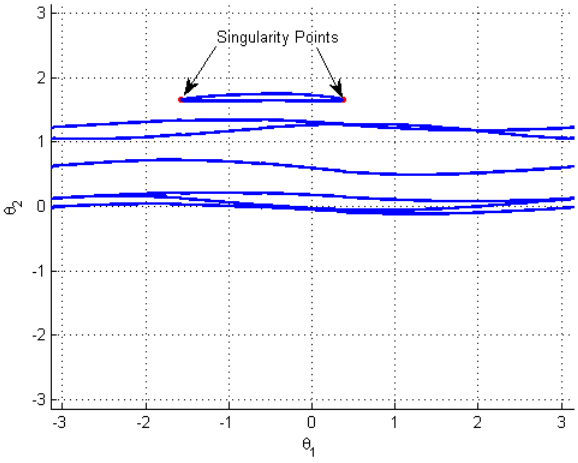

Figure 13: Trace of the motion curve for the double butterfly linkage, with $a_1 = 0.40$, projected onto the $\theta_1 - \theta_2$ plane.

remaining angles can be solved by using

$$\mathbf{T}_3 = \mathbf{R}_3/a_3, \tag{31}$$

$$\mathbf{T}_8 = \mathbf{R}_8/a_8, \tag{32}$$

$$\mathbf{T}_{11} = \mathbf{R}_{11}/a_{11}. \tag{33}$$

4.3 Singularity Points

The singularity condition for double butterfly linkage is

$$D := \det \begin{bmatrix} \frac{\partial H_3}{\partial \theta_2} & \frac{\partial H_3}{\partial \theta_4} & \frac{\partial H_3}{\partial \theta_7} \\ \frac{\partial H_8}{\partial \theta_2} & \frac{\partial H_8}{\partial \theta_4} & \frac{\partial H_8}{\partial \theta_7} \\ \frac{\partial H_{11}}{\partial \theta_2} & \frac{\partial H_{11}}{\partial \theta_4} & \frac{\partial H_{11}}{\partial \theta_7} \end{bmatrix} = 0. \tag{34}$$

Note that $\frac{\partial H_3}{\partial \theta_7} = 0$ since $\mathbf{T}_7$ does not appear in $\mathbf{R}_3$, and $\frac{\partial H_{11}}{\partial \theta_4} = 0$ since $\mathbf{T}_4$ does not appear in $\mathbf{R}_8$. The singularity points for double butterfly linkage are given by a system of equations consisting of the loop closure conditions Eq. (28)–(27) along with Eq. 34, To find singularity points at a given value of a_1, the system involves the following variable groups $\{\mathbf{T}_1, \mathbf{T}_2, \mathbf{T}_4, \mathbf{T}_7\}$,$\{\overline{\mathbf{T}}_1, \overline{\mathbf{T}}_2, \overline{\mathbf{T}}_4, \overline{\mathbf{T}}_7\}$.

4.4 Motion Curve

A trace of the motion curve with $a_1 = 0.198$ is projected onto the θ_1-θ_2 plane and shown in Fig. 12. This linkage has six circuits, with no singularities and six GIs for all values of θ_1. That is, the linkage can be assemvbled into six different configurations all having continuously rotating cranks. A trace of the motion curve with a slightly longer $a_1 = 0.40$ is projected onto the θ_1-θ_2 plane and shown in Fig. 13. This linkage has seven circuits, six of which have continously rotating cranks. Additionally, the seventh circuit exhibits two singularity points. Thus, eight GIs exist for $-1.5768 < \theta_1 < 0.3707$. A trace of the motion curve with a longer $a_1 = 2.50$ is projected onto the θ_1-θ_2 plane and shown in Fig. 14. This linkage has six circuits, one of which has a continously rotating crank. Of particular note is a circuit, where the linkage is able to rotate greater than one full revolution between singularities. This feature is seen as the "U" shape observed and noted in the motion trace of Fig. 14. Examples of this net-zero, singularity-free actuation that places the linkage into a different GI were identified for Stephenson III linkages in the previous section and in [1]. Those cases showed an "S" shape in the motion curve trace.

The final trace of the motion curve of a new double butterfly linkage with different parameters is projected onto the θ_1-θ_2 plane and shown in Fig. 15. This linkage has five circuits, none of which has a continously rotating crank. Of note is a circuit, where the linkage is also able to rotate greater than one full revolution between singularities. Again, a net-zero, singularity-free actuation that places the linkage into a different GI is identified. However, this appears as a closed curve where the turning points (singulaties) are separated by more than 360°.

4.5 Critical Points

The system to solve for the critical points of double butterfly linkage when a_1 considered the variable design parameter con-

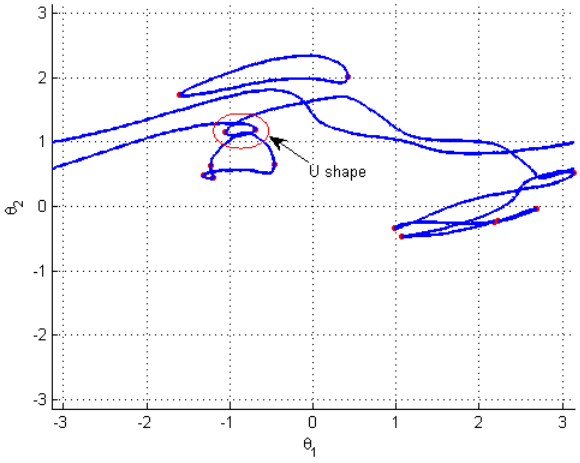

Figure 14: Trace of the motion curve for the double butterfly linkage, with $a_1 = 2.50$, projected onto the $\theta_1 - \theta_2$ plane.

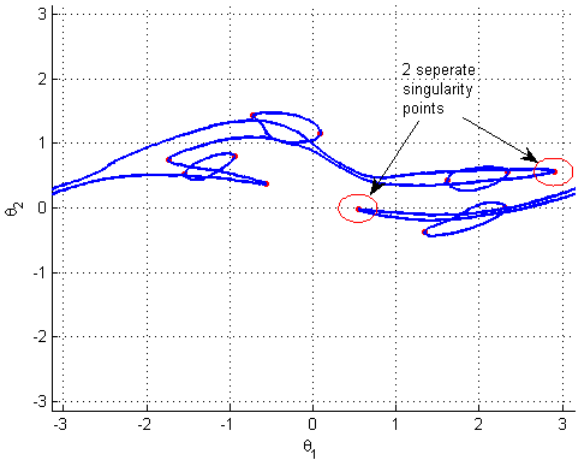

Figure 15: Trace of the motion curve for another double butterfly linkage with different parameters, projected onto the $\theta_1 - \theta_2$ plane.

sists of Eqs. (28)–(27),(34), and

$$E := \det \begin{bmatrix} \frac{\partial H_3}{\partial \theta_1} & \frac{\partial H_3}{\partial \theta_2} & \frac{\partial H_3}{\partial \theta_4} & \frac{\partial H_3}{\partial \theta_7} \\ \frac{\partial H_8}{\partial \theta_1} & \frac{\partial H_8}{\partial \theta_2} & \frac{\partial H_8}{\partial \theta_4} & \frac{\partial H_8}{\partial \theta_7} \\ \frac{\partial H_{11}}{\partial \theta_1} & \frac{\partial H_{11}}{\partial \theta_2} & \frac{\partial H_{11}}{\partial \theta_4} & \frac{\partial H_{11}}{\partial \theta_7} \\ \frac{\partial D}{\partial \theta_1} & \frac{\partial D}{\partial \theta_2} & \frac{\partial D}{\partial \theta_4} & \frac{\partial D}{\partial \theta_7} \end{bmatrix} = 0. \qquad (35)$$

Note that $\frac{\partial H_3}{\partial \theta_7} = 0$ since $\mathbf{T}_7$ does not appear in $\mathbf{R}_3$, and $\frac{\partial H_{11}}{\partial \theta_4} = 0$ since $\mathbf{T}_4$ does not appear in $\mathbf{R}_8$ .The system involves the following variables groups: a_1,$\{\mathbf{T}_1, \mathbf{T}_2, \mathbf{T}_4, \mathbf{T}_7\}$,$\{\overline{\mathbf{T}}_1, \overline{\mathbf{T}}_2, \overline{\mathbf{T}}_4, \overline{\mathbf{T}}_7\}$. However, the 4×4 matrix in Eq. (35) is very complicated and its determinant is more difficult to calculate than the examples presented above. A new approach to simplify the calculation is to combine the design parameter variable a_1 and its angle $\mathbf{T}_1$, $\overline{\mathbf{T}}_1$ by defining $\mathbf{X}_1 = a_1\mathbf{T}_1$ and $\overline{\mathbf{X}}_1 = a_1\overline{\mathbf{T}}_1$. Accordingly, the equation $\mathbf{T}_1\overline{\mathbf{T}}_1 - 1 = 0$ is eliminated from the system. The resulting variables groups are $\{\mathbf{X}_1, \mathbf{T}_2, \mathbf{T}_4, \mathbf{T}_7\}$,$\{\overline{\mathbf{X}}_1, \overline{\mathbf{T}}_2, \overline{\mathbf{T}}_4, \overline{\mathbf{T}}_7\}$. Thus, this method reduces one variable and one equation from system. The design parameter at critical points is determined as,

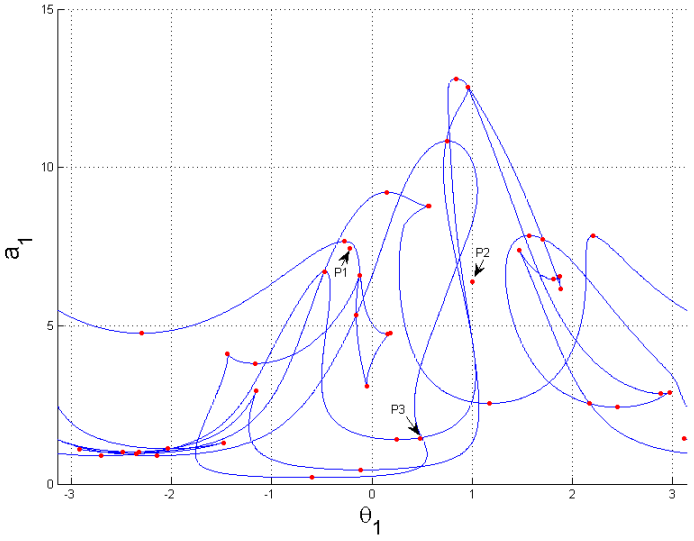

Figure 16: Double butterfly linkage singularity trace with respect to a_1.

$$a_1 = \sqrt{\mathbf{X}_1^2 + \overline{\mathbf{X}}_1^2} \qquad (36)$$

4.6 Singularity Trace

The singularity trace of double butterfly linkage with a variable a_1 is extremely convoluted and shown in Fig. 16. As before, the singularity trace separates the plot into regions having the same number of GIs. Solving the forward kinematic problem for one sample point within each zone determines the number in GIs in that entire zone. Additionally, sampling the motion curve between critical points that appear as smooth extrema determines the number of circuits.

There are three isolated critical points $P1$, $P2$ and $P3$ which do not lie on the singularity curve in Fig. 16. These critical points identify where a GI of the double butterfly linkage will lose a degree of freedom and become a fixed structure as indicated in Fig. 17.

A singularity trace of the double butterfly linkage with a

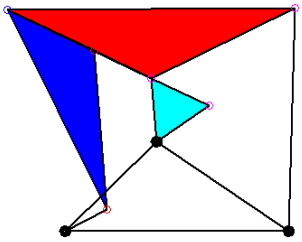

Figure 17: Double butterfly isolated critical position at P3.

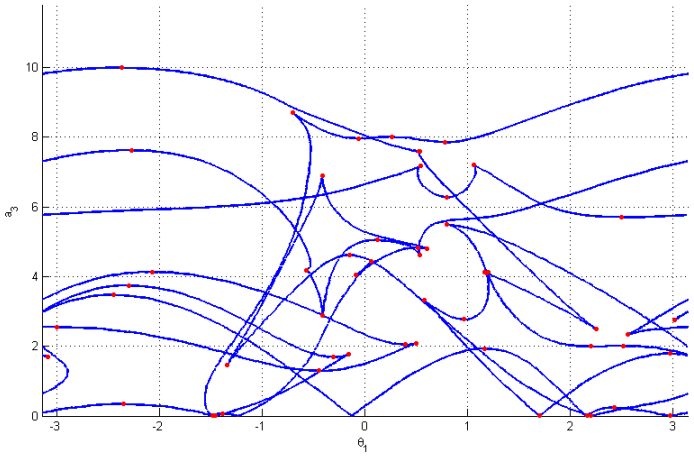

Figure 18: Double butterfly linkage singularity trace with respect to a_3.

variable a_3 is also convoluted and shown in Fig. 18. Similar to the singularity trace with respect to a_1, there are many cusps, and the cusps are related to a net-zero, singularity free activation sequence that places mechanism into a different GI.

5 Conclusions

This paper illustrated a general method for computing the forward kinematics, singularity points, critical points, motion curve and singularity trace for single-degree-of-freedom, closed-loop linkages with a designated input angle and one design parameter in this paper. The method was applied to a Watt II, Stephenson III and double butterfly linkages. Singularity traces for each linkage was constructed and analyzed. Several instances where the input angle is able to rotate more than one revolution between singularities were illustrated. Instances where presented where the singularity trace includes multiple coincident projections of the singularity curve. Additionally, isolated critical points were identified where the linkage configuration becomes a structure and looses the freedom to move.

REFERENCES

[1] Myszka D. Murray A. and Wampler C., 2012, Mechanism Branches, Turning Curves, and Critical Points, *Proceedings of IDETC/CIE 2012*, DETC2012-70277.

[2] McCarthy, J. M. and Soh, G.S., 2011, *Geometric Design of Linkages*, 2/e, Springer.

[3] Erdman, A. Sandor, G. and Kota, S., 2001, *Mechanism Design: Analysis and Synthesis*, Vol. 1, 4/e, Prentice Hall.

[4] Chase, T. and Mirth, J., 1993, Circuits and Branches of Single-Degree-of-Freedom Planar Linkages, *ASME Journal of Mechanical Design*, vol. 115, No. 2, pp. 223-230.

[5] Litvin, F. and Tan, J., 1989, Singularities in Motion and Displacement Functions of Constrained Mechanical Systems, *International Journal of Robot Research*, vol. 8, No. 2, pp. 30-43.

[6] Gosselin, C. and Angeles, J., 1990, Singularity Analysis of Closed-Loop Kinematic Chains, *IEEE Transactions on Robotics and Automation*, vol. 6, No. 3, pp. 281-290.

[7] Murray, A., Turner, M., Martin, D., 2008, Synthesizing Single DOF Linkages Via Transition Linkage Identification *ASME Journal of Mechanical Design*, Vol. 130, No. 2, 022301.

[8] Myszka, D., Murray, A., Schmiedeler, J., 2010, Using a Singularity Locus to Exhibit the Number of Geometric Inversions, Transitions and Circuits of a Linkage, *Proceedings of the ASME International Design Technical Conferences*, pp. 771-781.

[9] Wampler, C.W., 1999, Solving the Kinematics of Planar Mechanisms *ASME Journal of Mechanical Design*, Vol. 121, 387-391.

[10] Wampler, C.W., 1996, Isotropic Coordinates, Circularity, and Bezout Numbers: Planar Kinematics from a New Perspective, *Proceedings of the ASME Design Technical Conference*, Paper 96-DETC/MECH-1210.

[11] Wampler, C.W., and Sommese, A.J., 2011, Numerical Algebraic Geometry and Algebraic Kinematics, *Acta Numerica*, 469–567.

[12] Bates, D.J., Hauenstein, J.D., Sommese, A.J., and Wampler, C.W., Bertini: Software for Numerical Algebraic Geometry, available at http://www.nd.edu/∼sommese/bertini.